Three-Dimensional Visualization of Physiologically Based Kinetic Model Outputs

John Nichols,[1] Penny Rheingans,[2] Douglas Lothenbach,[1] Robert McGeachie,[3] Loren Skow,[3] and James McKim[1]

[1]Environmental Research Laboratory-Duluth, U.S. Environmental Protection Agency, Duluth, MN 55804 USA; [2]Martin Marietta, Inc., Research Triangle Park, NC 27709 USA; [3]Duluth Magnetic Resonance Imaging Center, St. Mary's Medical Center, Duluth MN 55805 USA

Outputs from a physiologically based toxicokinetic (PB-TK) model for fish were visualized by mapping time-series data for specific tissues onto a three-dimensional representation of a rainbow trout. The trout representation was generated in stepwise fashion: 1) cross-sectional images were obtained from an anesthetized fish using a magnetic resonance imaging system, 2) images were processed to classify tissue types and eliminate unnecessary detail, 3) processed images were imported to a visualization software package (Application Visualization System) to create a three-dimensional representation of the fish, encapsulating five volumes corresponding to the liver, kidney, muscle, gastrointestinal tract, and fat. Kinetic data for the disposition of pentachloroethane in trout were generated using a PB-TK model. Model outputs were mapped onto corresponding tissue volumes, representing chemical concentration as color intensity. The workstation software was then used to animate the images, illustrating the accumulation of pentachloroethane in each tissue during a continuous branchial (gill) exposure.
Key words: magnetic resonance imaging, physiologically based kinetic model, rainbow trout, three-dimensional visualization. *Environ Health Perspect* 102:952–956 (1994)

Physiologically based toxicokinetic (PB-TK) models are based on the anatomy, physiology, and biochemistry of the exposed organism and are used to generate chemical concentration time-course predictions for specific tissues and organs. This information can in turn be related to research on a compound's mechanism of action to improve understanding of relationships between applied dose and observed effect (*1–3*). In the last 25 years, PB-TK models have been developed to describe the disposition of more than 100 compounds in several mammalian species, including mice, rats, dogs, monkeys, and humans (*4–7*). PB-TK models are currently being used in human health risk assessment (*8,9*) and have been used to extrapolate kinetic information from rodents to humans (*10,11*).

Although more limited in scope than the mammalian modeling effort, progress has also been made toward developing PB-TK models for nonmammalian vertebrates, including fish. The first PB-TK models for fish were developed from intravascular infusion models for mice and were used to simulate the distribution of methotrexate in sting rays (*12*) and the distribution and elimination of phenol red in the dogfish shark (*13*). An intravascular infusion model was also developed to describe the distribution and elimination of pyrene in rainbow trout (*14*). Recently, improvements in understanding of chemical exchange across fish gills have led to the development of PB-TK models for waterborne organic chemicals. Branchial exposure models have been successfully used to simulate the kinetics of three chlorinated ethanes in rainbow trout (*15,16*) and channel catfish (*17*). Additional research has extended these models to include the dermal route of exposure (*18*). Simplified models have also been adapted for use with small fish such as the fathead minnow and Japanese medaka, which are the major contributors to the present aquatic toxicity database (*19,20*).

Despite their many advantages, however, there has been resistance to the use of PB-TK models. This resistance derives largely from the perception that these models are too complicated and therefore do not yield useful information. Consequently, individuals who could benefit from the use of PB-TK models do not use them. The purpose of this study was to develop the capability to visualize PB-TK model outputs. This was accomplished by mapping outputs from a PB-TK model for fish onto a three-dimensional representation of a rainbow trout.

All of the fish images presented in this paper were derived from one sexually immature male trout, weighing approximately 80 g. Several additional fish were used to refine the imaging technique. The trout were obtained from Seven Pines Fish Hatchery (Lewis, Wisconsin) and fed a daily maintenance diet (1.2% of body weight) of a commercial trout chow ("Silver Cup," Nelson and Sons, Inc., Murray, Utah). Feeding was suspended 24 hr before use of the trout.

The trout representation was generated in stepwise fashion using cross-sectional information obtained with a magnetic resonance imaging system (MRI; General Electric Signa; 1.5 Tesla). We anesthetized fish with tricaine methanesulfonate (MS 222) and placed them in a V-shaped plexiglass support filled with water. Images were acquired using a send–receive extremity coil and fast spin double echo technique. The dimensions of the coil limited the overall length of the fish to 180 mm. MRI settings were 3200 TR, 16 and 108 TE, 8 echo-train length, and a matrix of 256 × 192 with 1 average. Tissues in the first echo were distinguished primarily based on lipid content (Fig. 1a), whereas in the second echo differences between tissues reflect differences in water content (Fig. 1b). Slice thickness was set to 3 mm, with 1.5-mm spacing between slices to minimize interference due to residual signals from the previously excited slice. This provided an average (between mid-points) one-pass resolution of 6 mm. A scan of the entire fish yielded 30 slices and 60 total images (30 each of the first and second echoes). The MRI was then electronically offset by 3 mm, and a second image series was acquired, yielding a total of 60 slices (120 total echoes) at 3-mm resolution.

We acquired raw images using General Electric's digital file format. These were then converted to tagged image format files (TIFF) for importing to an image analysis software system (Image 1, Universal Imaging Corp., West Chester, Pennsylvania). All image processing was performed on the second of the two echoes obtained at each level, although in many cases the first echo was examined to confirm tissue types and boundaries. Images were magnified until individual pixels could be seen. We then used a contrast enhancement feature to assign each pixel a color hue depending on grey-scale intensity (Fig. 2). Tissues and organs were classified using a paintbrush option, which ascribed to each a unique numerical identifier (Fig. 3). Adipose tissue, which is distributed throughout the animal, was represented by the dorsal fat

Address correspondence to J. Nichols, U.S. EPA, 6201 Congdon Boulevard, Duluth, MN 55804 USA.
We thank St. Mary's Hospital and the staff of the Duluth Magnetic Resonance Imaging Center for their support, and Greg Lien and Steven Bradbury for critical reviews of the manuscript.
Received 19 May 1994; accepted 15 August 1994.

pad located just beneath the dorsal surface of the animal. The richly perfused compartment was represented by the stomach and intestinal tract (in the model this compartment also includes the pyloric ceca, spleen, and gonads). A portion of the poorly perfused compartment was given its own classification to create a representative muscle mass. The rest of this compartment, including the fins and skin, was classified with a different value, thereby defining both the compartment and the external surface of the animal. The water exterior to the fish and interior portions that did not correspond to a model compartment were classified as "other than fish."

We imported TIFFs for each of the 60 classified slices to a visualization software package [Application Visualization System (AVS), Advanced Visual Systems, Inc., Waltham, Massachusetts] running on a Silicon Graphics workstation (IRIS 480 VGX). The slices were then stacked to generate a three-dimensional volume containing the fish. Because sample spacing in the three dimensions was not uniform, the resulting volume was rectilinear. Accordingly, each volume element (voxel) was a rectilinear prism (0.78 × 0.59 × 3 mm) rather than a cube.

Six geometric representations were separately generated from the scan volume, one for each tissue compartment and one for the exterior surface of the fish. Voxels classified as a specific tissue type were isolated, and all other voxels were reclassified with the identifier 0. The single-feature volume was then blurred by convolution with a 3 × 3 × 3 voxel Gaussian convolution kernel. This blurring process reduced visual artifacts resulting from the rather large rectangular voxels. We generated the geometric representation by using a marching-cubes algo-

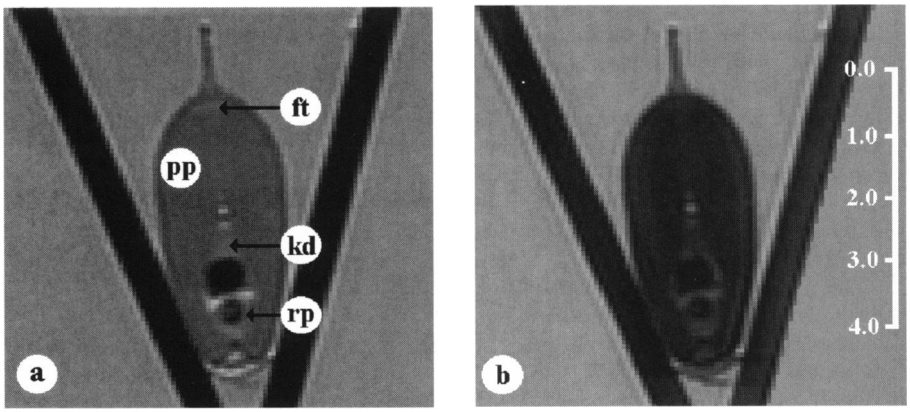

Figure 1. Cross-section of a rainbow trout obtained by magnetic resonance imaging. (a) First echo, highlighting differences in lipid content. (b) Second echo, highlighting differences in water content. Both echoes were obtained at the same level, approximately halfway down the length of the fish. ft, fat; pp, poorly perfused (represented by muscle); rp, richly perfused (represented by gastrointestinal tract); kd, kidney. The liver does not appear in this cross-section but can be readily identified in sections taken closer to the anterior end of the peritoneal cavity. The size of the fish is indicated by a centimeter scale in the second of the two echoes.

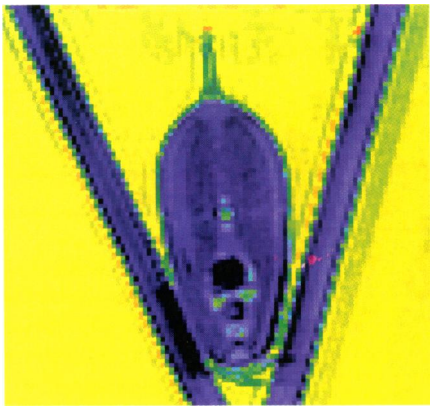

Figure 2. Color-enhanced cross-sectional image. The original image is shown in Figure 1b. The color hue of each pixel was assigned on the basis of grey-scale intensity.

Figure 3. Partially classified cross-sectional image. Tissues and organs were classified using a paintbrush utility. The fat, kidney, and portions of the gastrointestinal tract and poorly perfused tissue have been classified to illustrate the process.

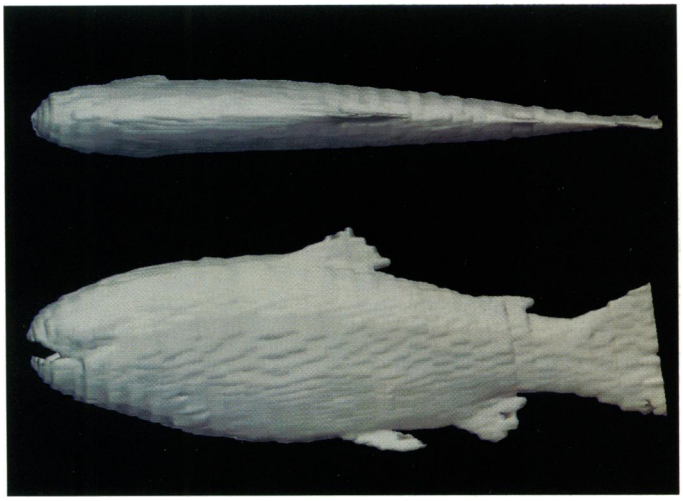

Figure 4. Top and side views of a rainbow trout reconstructed by Application Visualization System from 60 cross-sectional images.

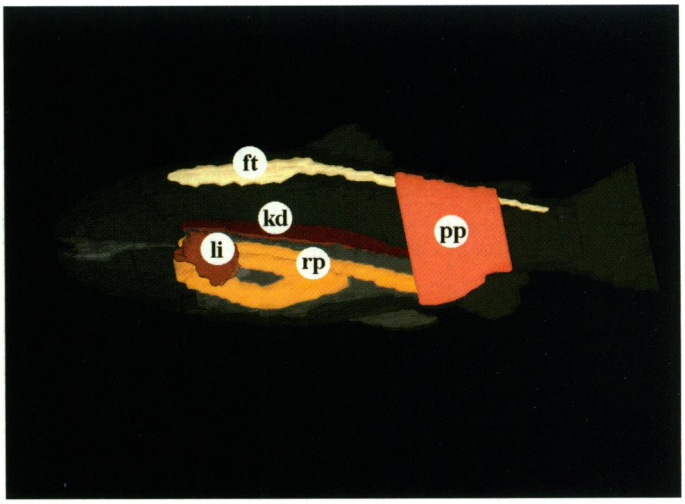

Figure 5. Side view of tissues and organs reconstructed by Application Visualization System from 60 cross-sectional images. ft, fat; pp, poorly perfused (represented by muscle); rp, richly perfused (represented by gastrointestinal tract); kd, kidney; li, liver.

rithm (*21*) to compute an isosurface at a value slightly below that of the tissue identifier. Finally, the five isosurfaces corresponding to each tissue, along with the isosurface showing the boundary between fish and "other than fish," were combined and rendered together (Figs. 4 and 5). The geometry-viewing facilities of AVS were used to control viewpoint, surface color, texture, opacity, and light position.

The disposition of pentachloroethane in rainbow trout was simulated using a PB-TK model running under Advanced Continuous Simulation Language (ACSL, Mitchell and Gauthier Associates Inc., Concord, Massachusetts) (Fig. 6). Similar predictions were previously shown to be in excellent agreement with observed residues when trout were exposed to pentachloroethane in water in a modified respirometer chamber (*15*). The model incorporates a counter-current description of chemical flux at fish gills (*22*). Chemical equilibrium is considered to exist between the tissues in each compartment and blood exiting the compartment (flow-limited distribution). The model was designed to reflect the physiology of fishes and includes portal blood flows to both the liver and kidney. Physiological and anatomical parameters were obtained from the literature (Table 1). Equilibrium chemical partition coefficients were estimated using an *in vitro* vial-equilibration technique (*23*).

We imported chemical time-course predictions for each of the model compartments to AVS as ASCII files. The data were then mapped onto corresponding tissue volumes, representing chemical concentration as the degree of color saturation. The three-dimensional rendering produced by AVS changes color at each time step as chemical concentrations change. The system can be used interactively by making parameter changes in the ACSL runtime environment. An output file is generated each time the model is run, which then serves as input for subsequent visualization efforts.

Hypothetical model outputs, in the form of an *X,Y* plot (Fig. 7), are compared to two corresponding screen images (Fig. 8) to illustrate how AVS can be used to visualize kinetic modeling outputs. After 2 hr of exposure, all tissues are colored to a similar degree (Fig. 8a). This is because differences in chemical partitioning to tissue are offset at early time points by differences in relative blood perfusion, resulting in similar chemical concentrations. With continued exposure (4 hr), differences in chemical partitioning begin to dictate the distribution pattern (Fig. 8b). At steady-state (>240 hr; image not shown), 75% of the total pentachloroethane burden is contained in the fat compartment, despite the fact that it composes only 9% of the mass of the animal.

Constraints on the publication of "hard copy" materials limit the presentation of visual computer output to a small number of static images. In the present study, the actual computer output consisted of 480 separate images (48 hr simulation/0.1 hr time-step). Approximately 30 sec were required to build each image when the

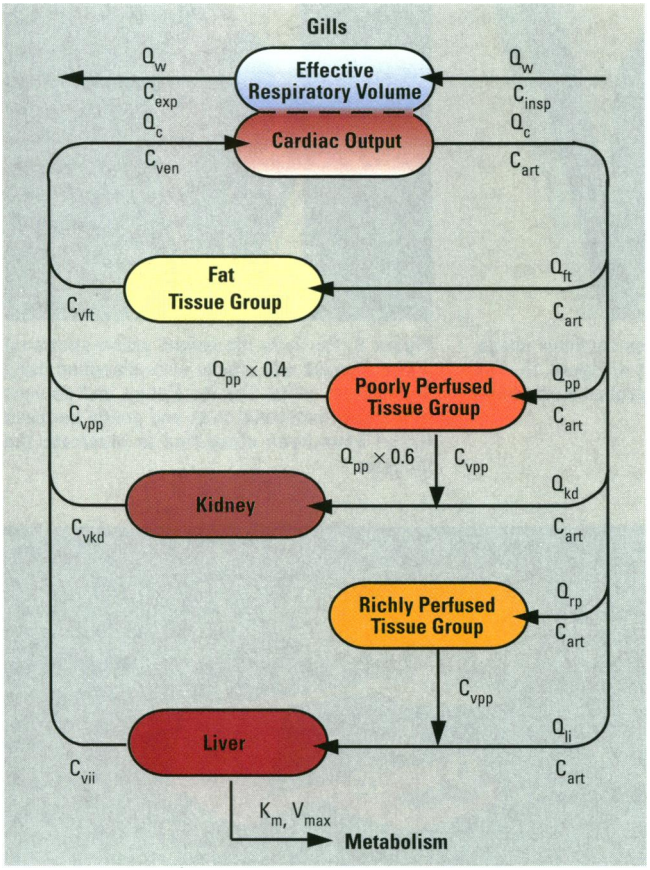

Figure 6. Schematic representation of a physiologically based toxicokinetic model for the uptake and disposition of waterborne organic chemicals in fish [adapted from Nichols et al. (*15*)]. Q_w, effective respiratory volume; C_{insp}, chemical concentration in inspired water; C_{exp}, chemical concentration in expired water; Q_c, cardiac output; Q_i, blood flow to tissues and organs (ft, fat; pp, poorly perfused; kd, kidney, rp, richly perfused; li, liver); C_{art}, chemical concentration in arterial blood; C_{ven}, chemical concentration in mixed venous blood; C_{vi}, chemical concentration in venous blood draining each tissue (tissue abbreviations are the same as those for blood flow); V_{max}, K_m, metabolic rate and capacity parameters.

Table 1. Physiological, metabolic, and partitioning parameters used in a physiologically based toxicokinetic model for rainbow trout exposed to pentachloroethane in water[a]

Parameter	Representation	Value
Physiological		
Body weight (kg)	BW	1.0
Ventilation volume (l/hr)	Q_v	10.6
Effective respiratory volume (l/hr)	Q_w	7.20
Oxygen consumption rate (mg O_2/hr)	VO_2	63.0
Cardiac output (l/hr)	Q_c	2.07
Arterial blood flow to tissues (l/hr)[b]		
Liver	Q_{li}	0.060
Fat	Q_{ft}	0.176
Poorly perfused	Q_{pp}	1.242
Richly perfused	Q_{rp}	0.476
Kidney	Q_{kd}	0.116
Tissue group volumes (l)		
Liver	V_{li}	0.012
Fat	V_{ft}	0.098
Poorly perfused	V_{pp}	0.818
Richly perfused	V_{rp}	0.063
Kidney	V_{kd}	0.009
Elimination rate and capacity		
Saturable kinetics (µg/kg, µg/kg-hr)	K_m, V_{max}	0.0, 0.0[c]
First-order kinetics (µg/kg-hr)	K_{fc}	0.0[c]
Equilibrium chemical partitioning		
Blood:water	P_{bw}	25.8
Liver:blood	P_{li}	2.83
Fat:blood	P_{ft}	85.8
Poorly perfused:blood	P_{pp}	3.22
Richly perfused:blood	P_{rp}	2.83
Kidney perfused:blood	P_{kd}	3.15

[a]From Nichols et al. (*15*). Values given are for a 1 kg trout at 12°C.

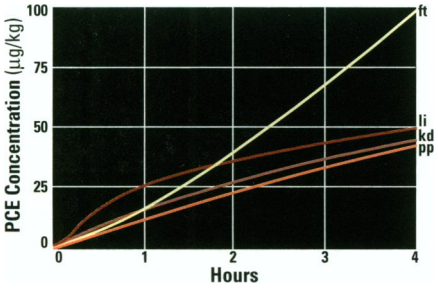

Figure 7. Simulated accumulation of pentachloroethane during a continuous inhalation exposure. ft, fat; pp, poorly perfused (represented by muscle); rp, richly perfused (represented by gastrointestinal tract); kd, kidney; li, liver. The concentration–time curve for the richly perfused compartment is nearly identical to that for the liver and is therefore not shown.

computer was in an interactive mode. These were saved as they were generated and were later used to produce animated output (10 frames/sec) using Silicon Graphic's "movie player" utility. The AVS "image viewer" can also be used to generate animated output; however, the lower performance of this utility (1.5 frames/sec) resulted in discernable breaks between images. Alternatively, images can be transferred to videotape for presentation using a conventional videocassette recorder.

The combined use of ACSL and AVS affords considerable flexibility for the development of visualization techniques in an interactive computing environment. The methods used are applicable to different animal species and are consistent with the compartmental structure of PB-TK models. It is anticipated that this or similar techniques could be used by modelers to communicate the results of their work to individuals who are not skilled in the interpretation of more conventional outputs. For example, those involved in chemical risk assessment are frequently required to extrapolate toxicological information from a surrogate species to the species of interest. Because they are based upon the biology of the organism, PB-TK models are uniquely well suited for this purpose. Nevertheless, the risk assessor may be unwilling or unable to use such models if the outputs are not understandable or cannot be easily communicated. Researchers who study basic mechanisms of toxic action can also benefit from the use of PB-TK models. This is because a PB-TK model yields chemical time-course predictions for the site of toxic action. *In vitro* observations can then be related to an environmental or occupational exposure, thereby establishing the toxicological relevance of the work. Finally, imaging techniques could be used to teach principles of kinetic modeling to students who might otherwise lack appreciation for (or interest in) the boxes and arrows that are typically used in schematic representations of model systems.

References

1. McKim JM, Nichols JW. Use of physiologically-based toxicokinetic models in a mechanistic approach to aquatic toxicology. In: Aquatic toxicology: molecular, biochemical, and cellular perspectives (Malins D, Ostrander G, eds). Boca Raton, FL:Lewis Publishers, 1994; 469–519.
2. Andersen ME. Tissue dosimetry in risk assessment or what's the problem here anyway? In: Pharmacokinetics in risk assessment, drinking water and health, vol 8. Washington, DC: National Academy Press, 1987;8–23.
3. Conolly RB, Reitz RH, Clewell HJ III, Andersen ME. Pharmacokinetics, biochemical mechanism and mutation accumulation: a comprehensive model of chemical carcinogenesis. Toxicol Lett 43:189–200 (1988).
4. Gerlowski LE, Jain RK. Physiologically based pharmacokinetic modeling: principles and applications. J Pharm Sci 72:1103–1127 (1983).
5. D'Souza RW, Boxenbaum H. Physiological pharmacokinetic models: some aspects of theory, practice and potential. Toxicol Ind Health 4:151–171 (1988).
6. Leung H-W. Development and utilization of physiologically based pharmacokinetic models for toxicological applications. J Toxicol Environ Health 32:247–267 (1991).
7. Krewski D, Withey JR, Ku L-F, Andersen ME. Applications of physiological pharmacokinetic modeling in carcinogenic risk assessment. Environ Health Perspect Suppl 102(8) (in press).
8. Andersen ME, Clewell HJ, Gargas HL, Smith FA, Reitz RH. Physiologically based pharmacokinetics and the risk assessment process for methylene chloride. Toxicol Appl Pharmacol 87:185–205 (1987).
9. Reitz RH, McCroskey PS, Park CN, Andersen ME, Gargas ML. Development of a physiologically based pharmacokinetic model for risk assessment with 1,4-dioxane. Toxicol Appl Pharmacol 105:37–54 (1990).
10. Ramsey JC, Andersen ME. A physiologically based description of the inhalation pharmacokinetics of styrene in rats and humans. Toxicol Appl Pharmacol 73:159–175 (1984).
11. Ward RC, Travis CC, Hetrick DM, Andersen ME, Gargas ML. Pharmacokinetics of tetrachloroethylene. Toxicol Appl Pharmacol 93:108–117 (1988).
12. Zaharko DS, Dedrick RL, Olivero VT. Prediction of the distribution of methotrexate in the sting rays *Dasyatidae sabina* and *sayi* by use of a model developed in mice. Comp Biochem Physiol 42:183–194 (1972).
13. Bungay PM, Dedrick RL, Guarino AM. Phamacokinetic modeling of the dogfish shark (*Squalus acanthias*): distribution and urinary and biliary excretion of phenol red and its glucuronide. J Pharmacokinet Biopharm 4: 377–388 (1976).
14. Law FCP, Abedini S, Kennedy CJ. A biologically-based toxicokinetic model for pyrene in rainbow trout. Toxicol Appl Pharmacol 110:390–402 (1991).
15. Nichols JW, McKim JM, Andersen ME, Gargas ML Clewell HJ III, Erickson RJ. A physiologically-based toxicokinetic model for the uptake and disposition of waterborne organic chemicals in fish. Toxicol Appl

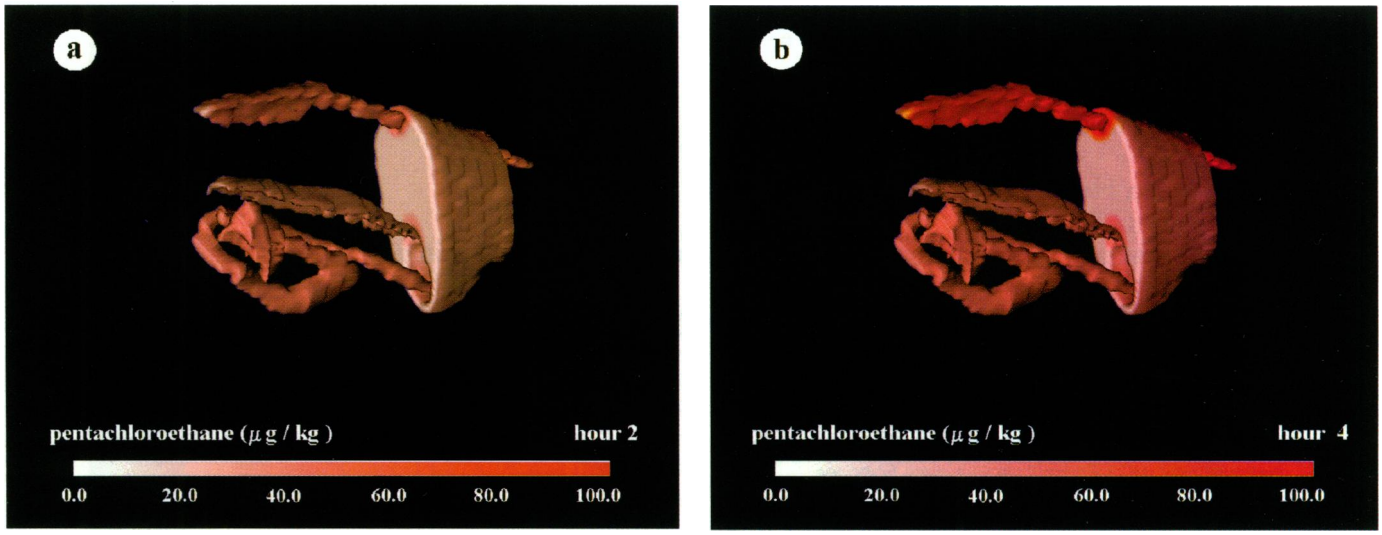

Figure 8. Accumulation of pentachloroethane after 2 hr (a) and 4 hr (b) of continuous branchial exposure. Concentrations in each tissue correspond to those shown in Figure 7.

Pharmacol 106:433–447 (1990).
16. Nichols JW, McKim JM, Lien GJ, Hoffman AD, Bertelsen SL. Physiologically-based toxicokinetic modeling of three waterborne chloroethanes in rainbow trout, *Oncorhynchus mykiss*. Toxicol Appl Pharmacol 110:374–389 (1991).
17. Nichols JW, McKim JM, Lien GJ, Hoffman AD, Bertelsen CL, Gallinat CA. Physiologically-based toxicokinetic modeling of three waterborne chloroethanes in channel catfish, *Ictalurus punctatus*. Aquat Toxicol 27:83–112 (1993).
18. McKim JM, Nichols JW, Lien GJ, Bertelsen SL. Kinetics of dermal uptake of three chloroethanes in rainbow trout (*Oncorhynchus mykiss*). Presented at the 11th annual meeting of the Society of Environmental Toxicology and Chemistry, Arlington, VA, 1990.
19. Lien GJ, McKim JM. Predicting branchial and cutaneous uptake of 2,2',5,5'-tetrachlorobiphenyl in fathead minnows (*Pimephales promelas*) and Japanese medaka (*Oryzias latipes*): rate limiting factors. Aquat Toxicol 27:15–32 (1993).
20. Lien GJ, Nichols JW, McKim JM, Gallinat CA. Modeling the accumulation of three waterborne chlorinated ethanes in fathead minnows (*Pimephales promelas*): a physiologically-based approach. Environ Toxicol Chem 13: 1195–1205 (1994).
21. Lorensen WE, Cline HE. Marching cubes: a high resolution 3D surface construction algorithm. Computer Graphic 21(4):163–169.
22. Erickson RJ, McKim JM. A model for exchange of organic chemicals at fish gills: flow and diffusion limitations. Aquat Toxicol 18:175–198 (1990).
23. Hoffman AD, Bertelsen SL, Gargas ML. An *in vitro* equilibration method for determination of chemical partition coefficients in fish. Comp Biochem Physiol 101:47–51 (1992).